

# Kinematic response analysis of piled foundations under seismic excitation

Rosa Maria Stefania Maiorano, Luca de Sanctis, Stefano Aversa, and Alessandro Mandolini

**Abstract:** This paper presents the results of an extensive parametric study on single piles and pile groups embedded in a two-layer subsoil profile, and is aimed to evaluate kinematic bending moments developing during earthquakes. A quasi three-dimensional finite element program has been used to perform dynamic analyses in the time domain. Piles have been considered as elastic beams, while the soil has been modelled using a linear elastic constitutive model. The aims of the paper are: (i) to evaluate kinematic bending moments in single piles and pile groups with dynamic analyses in the time domain, in different subsoil conditions; (ii) to review some existing design methods; (iii) to propose a simplified analysis procedure to evaluate maximum kinematic bending moments between two subsequent soil layers. The results of the dynamic analyses have shown that some of the simplified approaches provided in published literature tend to be conservative and can predict bending moments at the soil-layer interface with adequate accuracy only within certain depths of the soil layer interface. On the basis of the obtained results, a modified criterion to evaluate the transient peak bending moments at interfaces between layers is proposed.

*Key words:* kinematic interaction, single pile, pile groups, finite elements, seismic response.

**Résumé :** Cet article présente les résultats d'une étude paramétrique extensive sur des pieux simples et groupés insérés dans un sol de surface composé de deux couches. Cette étude avait comme objectif d'évaluer les moments de torsion cinématiques qui se développent pendant un séisme. Un programme d'éléments finis quasi tridimensionnels a été utilisé pour effectuer des analyses dynamiques dans le domaine temps. Les pieux ont été considérés comme des poutres élastiques, tandis que le sol a été modélisé à l'aide d'un modèle élastique constitutif linéaire. Les objectifs de cet article sont : (i) d'évaluer les moments de torsion cinématiques pour des pieux simples et groupés avec des analyses dynamiques dans le domaine temps, et ce pour différentes conditions de sol; (ii) de réviser quelques méthodes de conception existantes; (iii) de proposer une procédure simplifiée pour évaluer les moments de torsion cinématiques maximum entre deux couches subséquentes de sol. Les résultats des analyses dynamiques ont démontré que certaines approches simplifiées de la littérature ont tendance à être conservatrices et peuvent prédire les moments de torsion à l'interface entre les couches de sol de façon précise seulement pour quelques profondeurs de l'interface de la couche de sol. Selon les résultats obtenus, un critère modifié est proposé qui permet d'évaluer le moment de torsion maximum en régime transitoire à l'interface entre des couches de sol.

*Mots-clés :* interaction cinématique, pieu simple, pieux groupés, éléments finis, comportement sismique.

[Traduit par la Rédaction]

## Introduction

Dynamic soil pile interaction is a very complex problem involving a number of factors, such as soil profile, soil properties, nonlinear soil behaviour, seismically induced pore-water pressure, inertial effects, and kinematic interaction between soil and pile. Despite these complexities, engineering practice is still based on pseudostatic approaches and neglects the effects of kinematic interaction. In contrast, there is extensive

research on kinematic interaction, including field measurements (Gazetas et al. 1993; Nikolaou et al. 2001); in addition, pile damage confirming the role of kinematic bending moments has been observed after the earthquake events of Mexico City (Mexico) in 1985, Kobe (Japan) in 1995, and Chi Chi (Taiwan) in 1999. The importance of kinematic bending moments has been recently recognized by regulations such as Eurocode 8 (CEN/TC 250 2003b).

Studies on the kinematic response of pile foundations have been based on both simplified models (Dobry and O'Rourke 1983; Mylonakis 2001; Nikolaou et al. 2001; Sica et al. 2007) and more complex analyses in which the subsoil was assumed to be linear-elastic (Wu and Finn 1997a; Bentley and El Naggar 2000; Maiorano and Aversa 2006) or nonlinear (Wu and Finn 1997b; Maheshwari et al. 2005; Maiorano et al. 2007). Analyses based on simplified approaches have been essentially performed to define approximate analytical solutions capable of reproducing kinematic bending moments at the interface between two layers characterized by

Received 4 March 2008. Accepted 31 December 2008.  
Published on the NRC Research Press Web site at [cgj.nrc.ca](http://cgj.nrc.ca) on 7 May 2009.

**R.M.S. Maiorano, L. de Sanctis, and S. Aversa.**<sup>1</sup> Department of Technology, University of Napoli Parthenope, Centro Direzionale - Isola C4, 80143 Napoli, Italy.  
**A. Mandolini.** Department Civil Engineering, Second University of Napoli, Via Roma 29, 81031 Aversa (CE), Italy.

<sup>1</sup>Corresponding author (e-mail: [stefano.aversa@uniparthenope.it](mailto:stefano.aversa@uniparthenope.it)).

different shear moduli. On the other hand, studies based on advanced models have been performed to validate the applicability of analytical solutions. Most of these researches have been focused on the single pile problem. Published literature on dynamic pile group effects is much less extensive and is essentially dedicated to the elementary cases of shear modulus that is constant or linearly varying with depth (Fan et al. 1991; Maheshwari et al. 2004).

This paper reports kinematic pile–soil interaction analyses of both single piles and pile groups using a quasi three-dimensional (3D) finite element computer program (VERSAT-P3D, Wu 2006) to study the influence of a number of factors, such as the subsoil model and the soil properties, and to assess the applicability of simplified design methods available in published literature. Simplified subsoil conditions are considered, consisting of a two-layer profile with different values of the stiffness contrast between the two soil layers, in terms of their respective  $S$ -wave velocities  $V_{s2}/V_{s1}$ . Italian real acceleration-time histories are considered (Scasserra et al. 2006).

### Simplified design approaches

The simplest method of analysis for kinematic interaction is to assume that the pile follows the free-field soil motion, thus neglecting the interaction between pile and soil. Pile bending moments are then computed from the curvature of the horizontal displacements of the soil along a vertical line. This approach has been suggested by Margason and Holloway (1977) and is also recommended in some code provisions (Building Seismic Safety Council 2003). The bending moment at any depth  $z$  and time  $t$  can be computed as

$$[1] \quad M(z, t) = E_p I_p \frac{1}{R(z, t)}$$

where  $E_p I_p$  is the pile flexural rigidity and  $1/[R(z, t)]$  is the curvature of the vertical line. In the particular case of a homogeneous viscoelastic layer subjected to the passage of SH-propagating waves, the maximum curvature, according to Margason and Holloway (1977), is a function of the free-field soil acceleration,  $a_{ff} = a_{ff}(z, t)$ , and of the shear wave velocity,  $V_s$ :

$$[2] \quad \frac{1}{R(z, t)} = \frac{a_{ff}}{V_s^2}$$

In the case of layered soils, eq. [1] is inapplicable at interfaces between layers of different stiffness as the soil shear strain at these depths is discontinuous and consequently, the soil curvature is infinity. Soils are rarely homogeneous, thus the *free-field method* is not suitable in the majority of engineering problems. A number of closed-form expressions for a preliminary assessment of kinematic pile bending at the interface between two layers is available (Dobry and O'Rourke 1983; Nikolaou and Gazetas 1997; Mylonakis 2001; Nikolaou et al. 2001). The accuracy of these simplified criteria has been checked against some experimental evidence (Nikolaou et al. 2001) and benchmark solutions (Kaynia 1997; Mylonakis 2001) and at present time, such methods are commonly thought of as the most suitable

choice for engineering purposes. However, there are still significant limitations about their applicability, particularly under circumstances where the subsoil conditions do not meet the hypotheses on which the methods are based.

### Dobry and O'Rourke (1983) method

Dobry and O'Rourke (1983) developed a simple method for determining kinematic pile bending moments at the interface of two layers, modelling the pile as a beam on Winkler foundation (BWF) and assuming that

- (1) the soil in each layer is homogeneous, isotropic, and linearly elastic, characterized by their shear moduli  $G_1$  and  $G_2$
- (2) both layers are thick enough so that boundary effects outside the layers do not influence the response at the interface
- (3) the pile is long, vertical, and linearly elastic
- (4) perfect contact exists between the pile and the soil
- (5) each layer is subjected to a uniform static stress field,  $\tau$ , which generates constant shear strains ( $\gamma_1 = \tau/G_1$ ,  $\gamma_2 = \tau/G_2$ )
- (6) displacements are small

The explicit expression for the pile bending moment at the interface is

$$[3] \quad M = 1.86(E_p I_p)^{3/4} (G_1)^{1/4} \gamma_1 F$$

where

$$[4] \quad F = \frac{(1 - c^{-4})(1 + c^3)}{(1 + c)(c^{-1} + 1 + c + c^2)}$$

is a dimensionless function of the ratio of the shear moduli of the two layers and

$$[5] \quad c = \left( \frac{G_2}{G_1} \right)^{1/4}$$

The authors suggested to compute the peak shear strain  $\gamma_1$  in the first layer from a free-field response analysis. Alternatively, if the maximum acceleration,  $a_{\max, s}$ , is specified at the soil surface, as is usual when a seismic zonation is already available, the maximum shear strain could be evaluated by the approximate expression suggested by Seed and Idriss (1982):

$$[6] \quad \gamma_1 = \frac{r_d \rho_1 H_1 a_{\max, s}}{G_1}$$

where  $\rho_1$  and  $H_1$  are the density and the thickness of the upper layer, respectively, and  $r_d = r_d(z)$  is the well-known depth factor (Seed and Idriss 1982), that for preliminary design purposes can be assumed as

$$[7] \quad r_d = 1 - 0.015z$$

in which  $z$  is the depth in metres from the ground surface. It is to be noted that eq. [7] is not reliable for a depth in excess of approximately 15 m.

This method can predict the kinematic effects at any interface of a multi-layered soil profile, provided that the confining layers are thick enough.

**Nikolaou et al. (2001) method**

Nikolaou et al. (2001) derived a simplified expression for kinematic pile bending moments at the interface of two soil layers underlain by a rigid base. The pile is modelled as a beam on a dynamic Winkler foundation (BDWF) and the soil in each layer is assumed homogeneous, isotropic, and linearly elastic, with a constant soil-damping ratio. The expression for the interface bending moment has been derived by means of nonlinear regression of numerical data computed from a comprehensive parametric study carried out for a two-layer soil profile subjected to harmonic steady-state excitation.

This can be briefly reported as

$$[8] \quad M = 0.042\tau_C d^3 \left(\frac{L}{d}\right)^{0.30} \left(\frac{E_p}{E_1}\right)^{0.65} \left(\frac{V_{s2}}{V_{s1}}\right)^{0.50}$$

where  $\tau_C$  is a characteristic shear stress that is proportional to the actual shear stress that is likely to develop at the interface,  $L/d$  is the pile slenderness,  $E_p/E_1$  is the relative pile-soil stiffness, and  $V_{s2}/V_{s1}$  is the ratio of the shear-wave velocities of the two layers. Nikolaou et al. (2001) suggest to express  $\tau_C$  as a function of the maximum free-field acceleration at the soil surface:

$$[9] \quad \tau_C = a_{\max,s} \rho_1 H_1$$

Even though the method has been developed for harmonic excitations, it can be directly used in the time domain with the maximum acceleration  $a_{\max,s}$  of the soil surface obtained from a free-field response analysis.

The method does not consider any particular condition about the thickness of the two layers and is therefore applicable for any depth of the interface. Even though the authors recognize the importance of soil damping, all the analyses were performed using a pre-fixed value of  $D = 10\%$  and no sensitivity study was performed.

**Mylonakis (2001) method**

Another simplified method for predicting the kinematic bending moment at the interface between two layers was developed by Mylonakis (2001). This method is fundamentally different from the one by Nikolaou et al. (2001) as it is not based on a curve-fitting of numerical data, but on the response analysis of a mechanistic model. The basic assumptions are the same as those of the Dobry and O'Rourke (1983) method. The improvements with reference to the Dobry and O'Rourke method are

- (1) the seismic excitation is a harmonic horizontal displacement imposed at the bedrock
- (2) both radiation and material damping are accounted for
- (3) soil layers are thick, but not unbounded

The maximum bending moment can be compactly expressed as

$$[10] \quad M = \frac{(E_p I_p)(\varepsilon_p/\gamma_1) \phi}{r} \gamma_1$$

where  $\gamma_1$  is the peak shear strain in the upper layer at the interface depth,  $r$  is the pile radius, and  $\varepsilon_p/\gamma_1$  is the static strain transfer function that can be expressed according to the theoretical solution

$$[11] \quad \frac{\varepsilon_p}{\gamma_1} = \frac{1}{2c^4} (c^2 - c + 1) \left(\frac{H_1}{d}\right)^{-1} \times \left\{ \left[ 3 \left(\frac{k_1}{E_p}\right)^{1/4} \left(\frac{H_1}{d}\right) - 1 \right] c(c-1) - 1 \right\}$$

with  $k_1$  being the soil-spring stiffness according to Kavvasdas and Gazetas (1993)

$$[12] \quad k_1 = \delta E_1$$

where

$$[13] \quad \delta = \frac{3}{1-\nu^2} \left(\frac{E_p}{E_1}\right)^{-1/8} \left(\frac{L}{d}\right)^{1/8} \left(\frac{H_1}{H_2}\right)^{1/12} \left(\frac{G_1}{G_2}\right)^{-1/30}$$

where  $H_2$  is the thickness of lower layer and  $\nu$  is the Poisson's ratio. The coefficient  $\phi$  in eq. [10] is an amplification factor accounting for the effect of the dynamic nature of the excitation on the strain transfer function. As highlighted by Mylonakis (2001), this coefficient is usually less than 1.25. At a preliminary stage of the study on the kinematic response of a piled foundation, this coefficient ( $\phi = 1$ ) can be neglected without any particular implication.

If the seismic excitation is specified at an elevation below the interface, Mylonakis suggests to perform a free-field analysis to estimate the peak shear strain  $\gamma_1$ . Alternatively, it is suggested to use eq. [6] by Seed and Idriss (1982), which, however, is valid for relatively shallow depths, as it focuses on liquefaction phenomena more than soil foundation interaction.

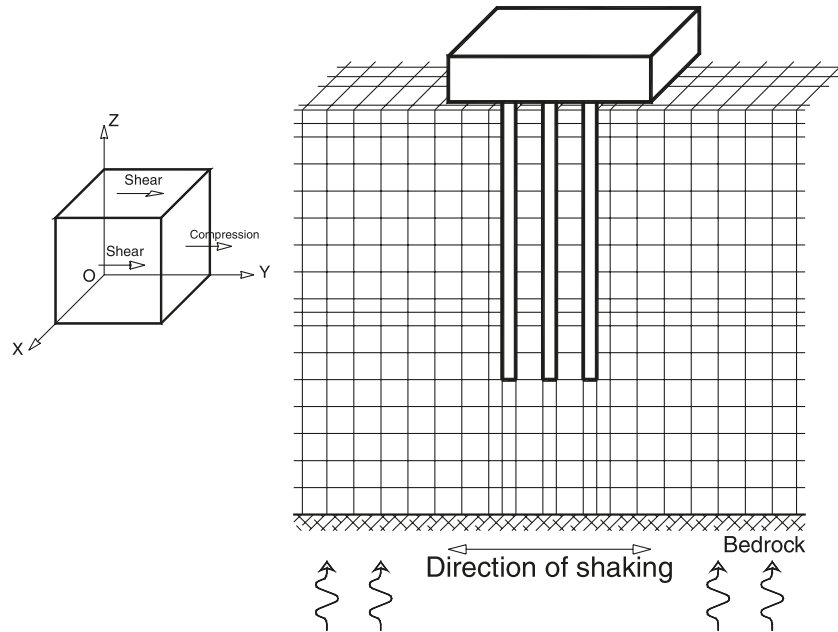
**Numerical model for dynamic analysis**

The numerical model used for the parametric study, VERSAT-P3D version 2006 (Wu 2006), is an enhancement of the quasi-3D finite element methods developed by Wu and Finn (1997a, 1997b) including the use of an eight-node pile element and energy-transmitting boundaries (Lysmer and Kuhlemeyer 1969).

Under vertically propagating shear waves (Fig. 1), the soil primarily undergoes shearing deformations in the X-Y plane, except in the area near the pile where extensive compression deformations develop in the direction of shaking. The compression deformations also generate shearing deformations in the Y-Z plane. Therefore, assumptions are made that the dynamic response is governed by the shear waves in the X-Y and Y-Z planes and the compression waves in the direction of shaking, Y. Deformations in the vertical direction and normal to the direction of shaking are neglected. Comparisons with full 3D elastic solutions confirm that these deformations are relatively unimportant for horizontal shaking (Wu and Finn 1997b). Piles are modelled using the ordinary Eulerian beam theory. Bending of piles occurs only in the direction of shaking. Dynamic soil pile interaction is maintained by enforcing displacement compatibility between the pile and the soil. An eight-node brick element is used to represent soil and an eight-node beam element is used to simulate the piles.

The global dynamic equilibrium equations are written in matrix form as

Fig. 1. Principle of the quasi-3D dynamic analysis of the pile–soil–structure interaction (after Wu and Finn 1997a, 1997b).



$$[14] \quad [M]\{\ddot{v}\} + [C]\{\dot{v}\} + [K]\{v\} = -[M]\{I\}\ddot{v}_0(t)$$

in which  $\ddot{v}_0(t)$  is the base acceleration,  $\{I\}$  is a unit column vector, and  $\{\ddot{v}\}$ ,  $\{\dot{v}\}$ , and  $\{v\}$  are the nodal acceleration, velocity, and displacement, respectively.  $[M]$ ,  $[C]$ , and  $[K]$  are the mass, damping, and stiffness matrices, respectively. Direct step-by-step integration using the Wilson  $\theta$  method is employed to solve eq. [14].

The damping is of the Rayleigh type, which is both mass and stiffness dependent. The damping matrix  $[C]$  for a soil element is given by

$$[15] \quad [C] = D \left( \frac{8}{5} \omega_1 [M] + \frac{[K]}{\omega_1} \right)$$

where  $\omega_1$  is the fundamental circular frequency of the pile–soil system obtained by solving the corresponding eigenvalue problem and is updated with time. The hysteretic damping ratio,  $D$ , is a function of element shear strain (Seed et al. 1986). Equation [15] provides a damping ratio,  $D$ , approximately constant between two frequencies  $\omega_1$  and  $n\omega_1$  ( $n = 4$ ).

The accuracy of the VERSAT-P3D code has been checked against more rigorous solutions obtained by the boundary integral method for harmonic-type excitations (Fan et al. 1991). Finn (2005) has reported a back-analysis of the dynamic response of a single-pile prototype in a centrifuge test. He found that the code was capable of reproducing the observed behaviour at a reasonable level.

## Parametric study

Kinematic interaction analyses have been performed for pile groups and isolated piles embedded in an ideal subsoil consisting of two layers underlain by a rigid base (Fig. 2). This base was located at a depth  $H = 30$  m while the interface between the layers ( $H_1$ ) was located at variable depths (5, 10, 12, 15, 17, and 19 m).

The shear-wave velocity of the upper layer,  $V_{s1}$ , was taken as 50 or 100 m/s, while the ratio of the two shear-wave velocities was set equal to 2 and 4 for both values of  $V_{s1}$ . Finally, a soil density,  $\rho$ , of 1.94 Mg/m<sup>3</sup> and a Poisson's ratio  $\nu = 0.4$  have been assumed, to compare the results with those obtained by Nikolaou et al. (2001). The well-known relation between the shear-wave velocity and the small-strain shear modulus  $G_0$  is

$$[16] \quad V_s(z) = \sqrt{\frac{G_0(z)}{\rho}}$$

Table 1 summarizes the subsoil models together with the geotechnical parameters of the soils and the corresponding equivalent velocity

$$[17] \quad V_{s,30} = \frac{30}{\sum_{i=1,n} h_i/V_{s,i}}$$

defined by Eurocode EN 1998–1 (CEN/TC 250 2003a).

The resulting soil profiles can be classified as ground type D, and sometimes ground type C, according to EN-1998–1 (CEN/TC 250 2003a). Piles with a length  $L = 20$  m, a diameter  $d = 0.6$  m, and a Young's modulus  $E_p = 25$  GPa were considered. The pile head was fixed against rotation. A  $3 \times 3$  or alternatively a  $5 \times 5$  pile group was considered. The pile spacing was taken equal to four diameters. In a few cases (G4–2 and G4–4) the pile spacing was also set equal to  $2.5d$ . A number of 144 analyses were performed.

Linear elastic analyses were performed in the time domain; a damping ratio  $D = 10\%$  was assumed for the soil layers to compare the results with those of the simplified approaches (Nikolaou et al. 2001). Input acceleration time histories were selected from a database of records of Italian seismic events (Scasserra et al. 2006). The signals were scaled to values of  $a_g$  equal to  $0.35g$  that would be expected

**Fig. 2.** Cases considered in the parametric study.

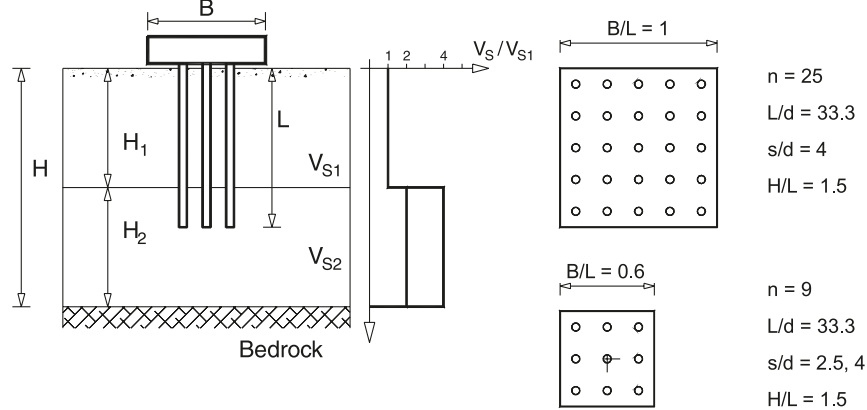


**Table 1.** Parametric cases and geotechnical parameters of the soils.

Subsoil	Case	$V_{s1}$ (m/s)	$V_{s2}/V_{s1}$	$H_1/L$	$E_p/E_1$	$V_{s,30}$ (m/s)	Ground type*
S1	S1-1	50	2	0.25	1841	86	D
	S1-2	50	2	0.50	1841	75	D
	S1-3	50	2	0.60	1841	71	D
	S1-4	50	2	0.75	1841	67	D
	S1-5	50	2	0.85	1841	64	D
	S1-6	50	2	0.95	1841	61	D
	S1-7	50	2	1.00	1841	60	D
S2	S2-1	50	4	0.25	1841	133	D
	S2-2	50	4	0.50	1841	100	D
	S2-3	50	4	0.60	1841	91	D
	S2-4	50	4	0.75	1841	80	D
	S2-5	50	4	0.85	1841	74	D
	S2-6	50	4	0.95	1841	69	D
	S2-7	50	4	1.00	1841	67	D
S3	S3-1	100	2	0.25	460	171	D
	S3-2	100	2	0.50	460	150	D
	S3-3	100	2	0.60	460	143	D
	S3-4	100	2	0.75	460	133	D
	S3-5	100	2	0.85	460	128	D
	S3-6	100	2	0.95	460	122	D
	S3-7	100	2	1.00	460	120	D
S4	S4-1	100	4	0.25	460	267	C
	S4-2	100	4	0.50	460	200	C
	S4-3	100	4	0.60	460	182	C
	S4-4	100	4	0.75	460	160	D
	S4-5	100	4	0.85	460	148	D
	S4-6	100	4	0.95	460	138	D
	S4-7	100	4	1.00	460	133	D

\*Classified according to EN-1998-1 (CEN/TC 250 2003a).

in a zone of high seismicity according to Italian seismic classification (Presidenza del Consiglio dei Ministri 2003), and have been applied to the base of the subsoil models. Table 2 summarizes the main data (seismic event, magnitude, peak ground acceleration (PGA), location of the recording station, distance from the epicentre) of the acceleration time histories used in the analyses (Fig. 3).

**Selected analysis results**

Some selected results of the finite element (FE) simulations performed for a small group (3 × 3), with pile spacing

$s/d$  equal to 2.5 and 4 in the case S4-4 and Tolmezzo earthquake (A-TMZ000) are reported in Fig. 4. The distributions of bending moment envelopes are reported for edge piles (A, D, and E) in Fig. 4a ( $s/d = 4$ ) and for central pile B in Fig. 4b (for both  $s/d = 2.5$  and 4).

For comparison, the bending-moment profile computed for the single pile has been added to both Figs. 4a and 4b. The maximum deflection and acceleration profiles along the central pile and a vertical axis located at 4.8 m from the centre of the foundation are reported in Figs. 4c and 4d, respectively ( $s/d = 4$ ). A free-field analysis in the same subsoil condition was also performed by using the EERA code

**Table 2.** Acceleration time-histories used in the analyses.

Name	Event	Station	$M_w$	Distance (km)	PGA (g)
A-TMZ000	Friuli, 1976	Tolmezzo	6.5	23	0.357
E-NCB090	Umbria-Marche, 1997	Norcia Umbra	5.5	10	0.382

**Fig. 3.** Acceleration time histories and response spectra at the bedrock roof.

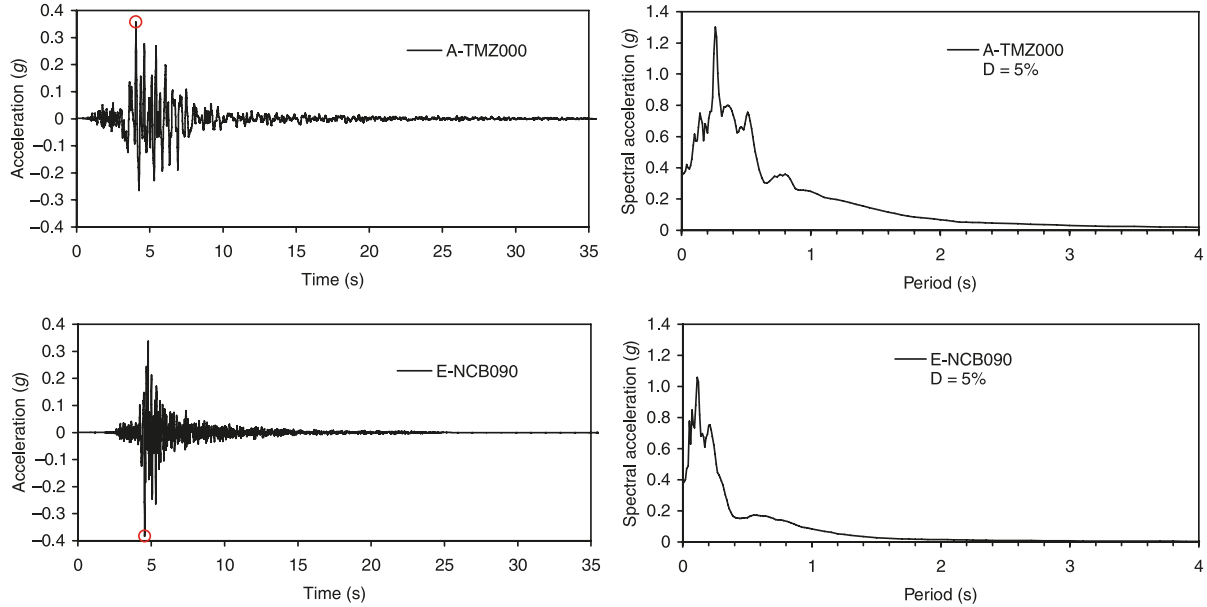
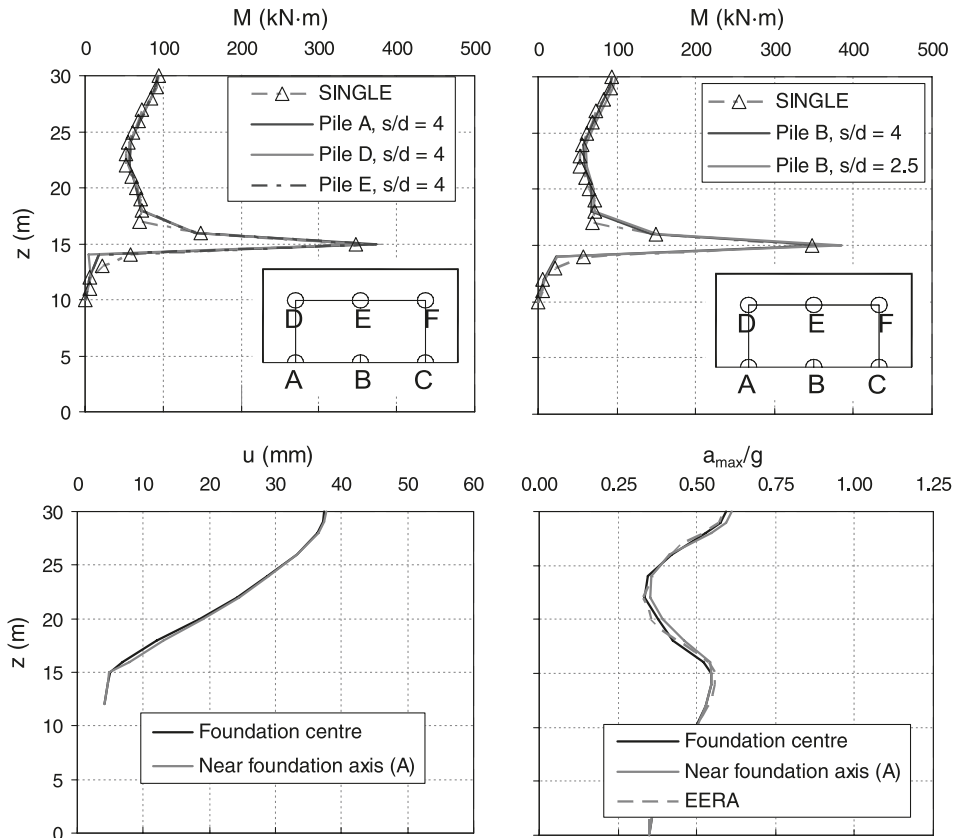


**Fig. 4.** Results for subsoil S4-4 case ( $V_{s2}/V_{s1} = 4$ ,  $V_{s1} = 100$ , and  $H_1 = 75\%L$ ) and Tolmezzo earthquake. EERA, Bardet et al. (2000).



(Bardet et al. 2000); the corresponding acceleration profile is reported in Fig. 4d for comparison.

At the interface depth, the bending moment envelope exhibits a pronounced peak while the pile-deflection curves are less affected by the transition from the upper to the lower layer. It may be seen that no significant differences exist between the bending moment profiles of the piles belonging to the group ( $s/d = 4$ ). The effects of pile spacing also appear to be negligible. At the same time the response of these piles is practically coincident with that found for the single pile. In other terms the (kinematic) group effects can be considered negligible, at least in the case of small pile groups and linear elastic behaviour of soil. Such results, and many similar findings not presented for lack of space, seem very appealing as they indicate that the kinematic effect of a pile group can be predicted with reasonable accuracy by merely performing a single-pile analysis; this implies, in turn, considerable savings in terms of computational efforts. This result is in agreement with the field measurements on a 12-storey building in Japan carried out by Nikolaou et al. (2001) and the analytical studies of Fan et al. (1991) and Kaynia and Mahzooni (1996).

A synthesis of the results obtained for subsoils S3 and S4 ( $V_{s1} = 100$  m/s), is illustrated in Fig. 5, where the maximum bending moments at the interface depth ( $M_{INT}$ ) and at the pile top ( $M_{CAP}$ ) are plotted against  $H_1$ . The continuous lines refer to analyses performed for a ( $3 \times 3$ ) group of piles spaced at  $s/d = 4$ , and particularly to pile A belonging to the middle row (see Figs. 4a and 4b), while the dashed lines pertain to the single pile. The following deductions about Fig. 5 are worthy of note:

- (1) The response of the single pile remains practically unchanged in the group whatever the value taken by  $H_1$ .
- (2) The bending moments  $M_{INT}$  are strongly affected by the ratio of the two shear wave velocities.
- (3) For both Tolmezzo and Norcia Umbra earthquake, the plot of  $M_{INT}$  is more variable for larger values of  $V_{s2}/V_{s1}$ .
- (4) The  $M_{CAP}$  bending moments tend to converge for increasing values of  $H_1$ , where the effect of the interface depth is of minor concern and the bending moment at the pile cap is essentially governed by the elastic properties of the upper layer.

The results found for subsoils S1 and S2 ( $V_{s1} = 50$  m/s) are illustrated in Fig. 6 and lead to similar conclusions.

### Analysis results versus simplified methods

In Figs. 7 and 8, the kinematic bending moments at the interface of the two layers obtained from the FE analyses are compared with those evaluated through the simplified methods, for different values of the interface depth  $H_1$ . Simplified formulas have been applied after performing a free-field response analysis by the EERA code. The maximum acceleration at the soil surface provided by the EERA code has been employed in the expression of Seed and Idriss (1982) (eq. [6]) to obtain the peak shear strain at the interface  $\gamma_1$  and then, again, in eq. [9] to derive the maximum characteristic shear stress  $\tau_c$ . For simplicity, the method by Mylonakis (2001) has been applied with  $\Phi = 1$ .

It is worthy of note that the assessment of kinematic

bending moments via  $a_{\max,s}$  at the soil surface represents the most widespread application criterion for the simplified formulas, because the maximum acceleration at the soil surface is usually available in practice, as a result of local seismic zonation studies or because it is imposed by the existing seismic codes or classifications.

The comparisons in Figs. 7 and 8 show that:

- (1) the simplified solutions do not significantly differ with each other and tend to be conservative
- (2) there are significant discrepancies between the bending moments predicted by the finite element analyses ( $M_v$ ) and those evaluated by the simplified expressions ( $M$ ), especially for decreasing values of  $V_{s1}$  (or increasing  $E_p/E_f$ ) and increasing values of  $H_1$ , with a maximum ratio of  $M_v/M$  of about 2.4
- (3) the bending moments obtained by the simplified expressions increase for increasing values of the interface depth, whereas those computed by the finite element analyses exhibit a sort of “plateau”

The simplified expressions could be applied with reasonable accuracy only for certain depths of the interface between the two layers ( $H_1 < 50\%L$ ) and moderate values of the pile-soil relative stiffness. In contrast, considerable discrepancies are expected for higher values of  $H_1$ , i.e., in the case of end-bearing piles, which is quite frequent in engineering practice.

### Modified criterion to evaluate the maximum kinematic bending moments

The method by Dobry and O'Rourke (1983) is based on a number of simplified assumptions, such as the nature of loading that was supposed pseudostatic, and the thickness of the layers that were considered “unbounded,” so that boundary effects at the pile tip and head do not influence the kinematic response at the interface. It is therefore not surprising that the method fails to predict the kinematic bending moments, especially in the case where the interface is located in the proximity of the pile tip.

The effect of the finite thickness of the two layers was incorporated into the improved model developed by Mylonakis (2001) and into the parametric studies carried out by Nikolaou et al. (2001). Indeed, the theoretical solution by Mylonakis (2001) is based on the assumption of “thick” layers, i.e., layers with a thickness greater than the so-called active pile length (Randolph 1981; Pender 1993) allowing the pile to be modelled as a semi-infinite beam with essentially no error; this is a fundamental hypothesis introduced by Mylonakis (2001) to ensure a finite response at a large distance from the interface. On the other hand, the closed-form expression developed by Nikolaou et al. (2001) is based on a BDWF model in which the interface was located at  $1/2L$  or alternatively  $2/3L$ . In both situations, therefore, the case with the interface in the vicinity of the pile tip has not been adequately addressed; this may explain, in turn, the disagreement between the bending moments computed by the finite element analyses and those evaluated by the closed-form expressions for  $H_1$  within the active pile length or larger than  $2/3L$ . Significant differences, however, have

**Fig. 5.** Maximum bending moments in the case  $V_{s1} = 100$  m/s (subsoils S3 and S4) for a  $(3 \times 3)$  pile group and a single pile.

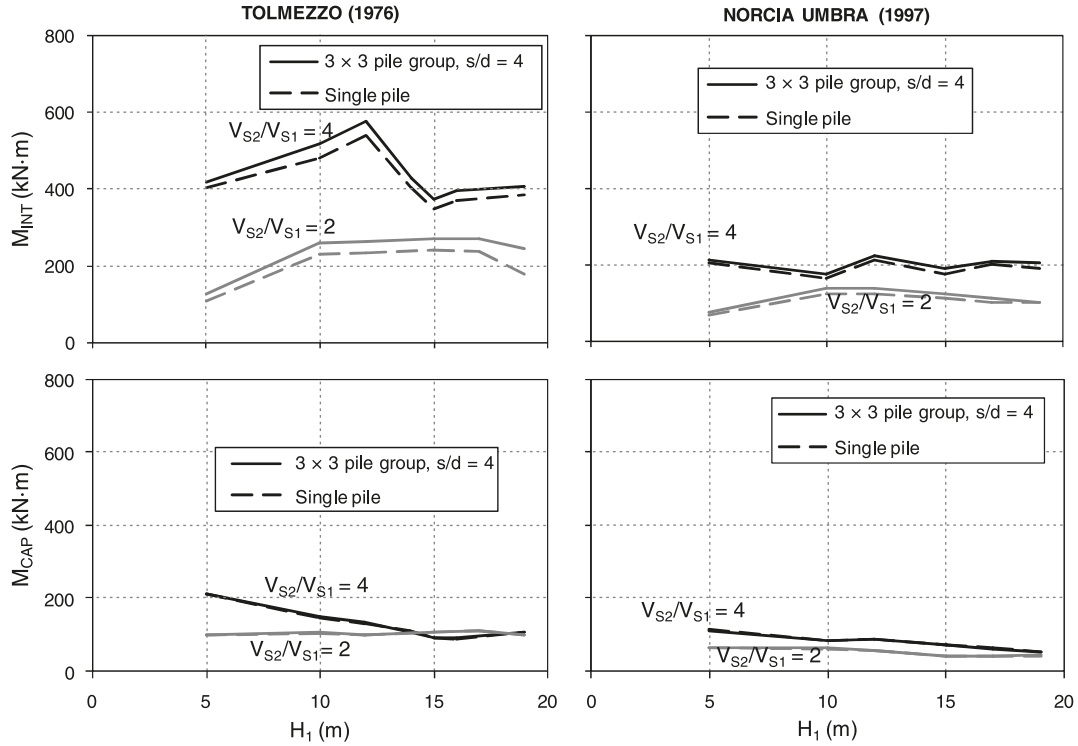
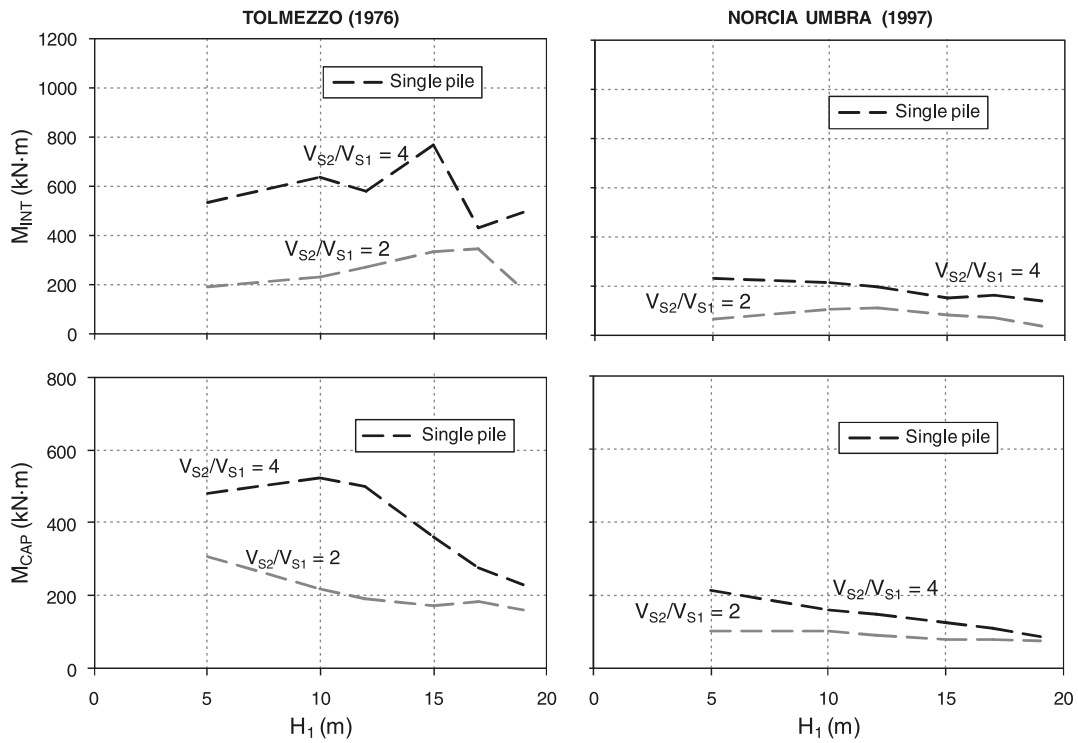


**Fig. 6.** Maximum bending moments in the case  $V_{s1} = 50$  m/s (subsoils S1 and S2) for a single pile.



been also detected for intermediate values of  $H_1$  and particularly in the case of  $V_{s1} = 50$  m/s (see Fig. 8).

The point of major concern is probably the evaluation of the peak shear strain at the interface or the characteristic shear stress. As an example, Fig. 9 shows the comparison between the characteristic shear stresses computed via

eq. [9] and the maximum shear stresses at the interface directly evaluated by the EERA code in the case  $V_{s1} = 100$  m/s. It can be seen that the curves are significantly different. The maximum shear strain at the interface directly evaluated by a free-field response analysis is almost constant with increasing values of  $H_1$  and is very similar in shape to



**Fig. 7.** Comparison between bending moments predicted by analytical solutions and those evaluated by the finite element analyses for subsoils S3 and S4 ( $V_{S1} = 100$  m/s).

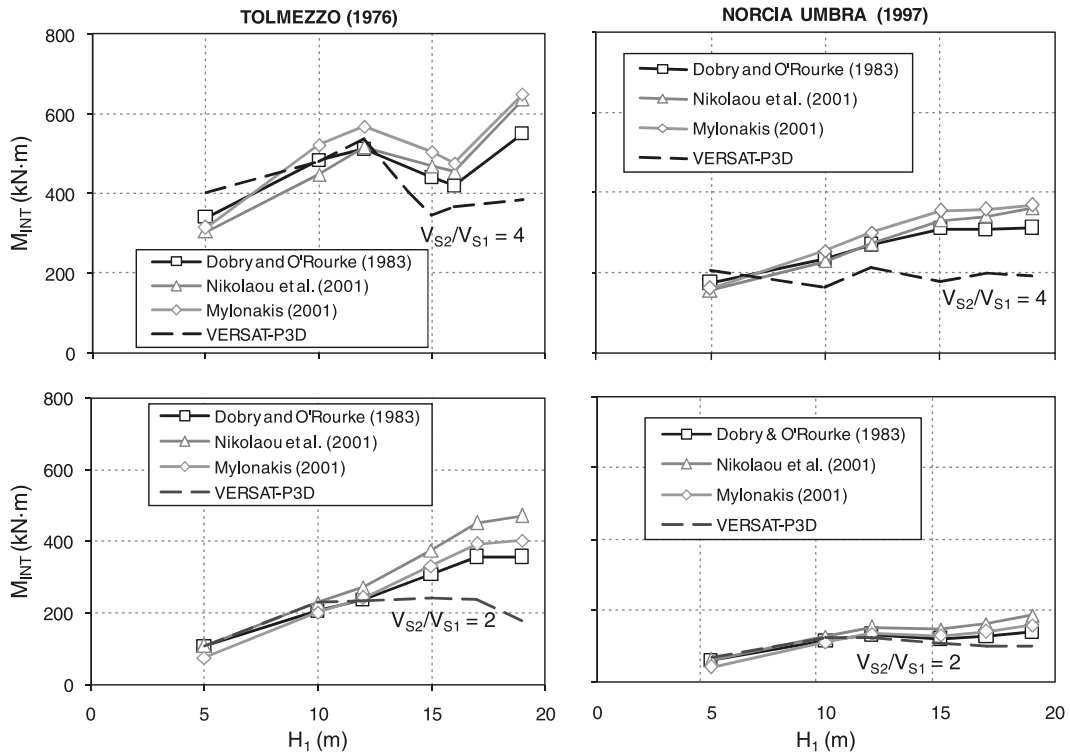
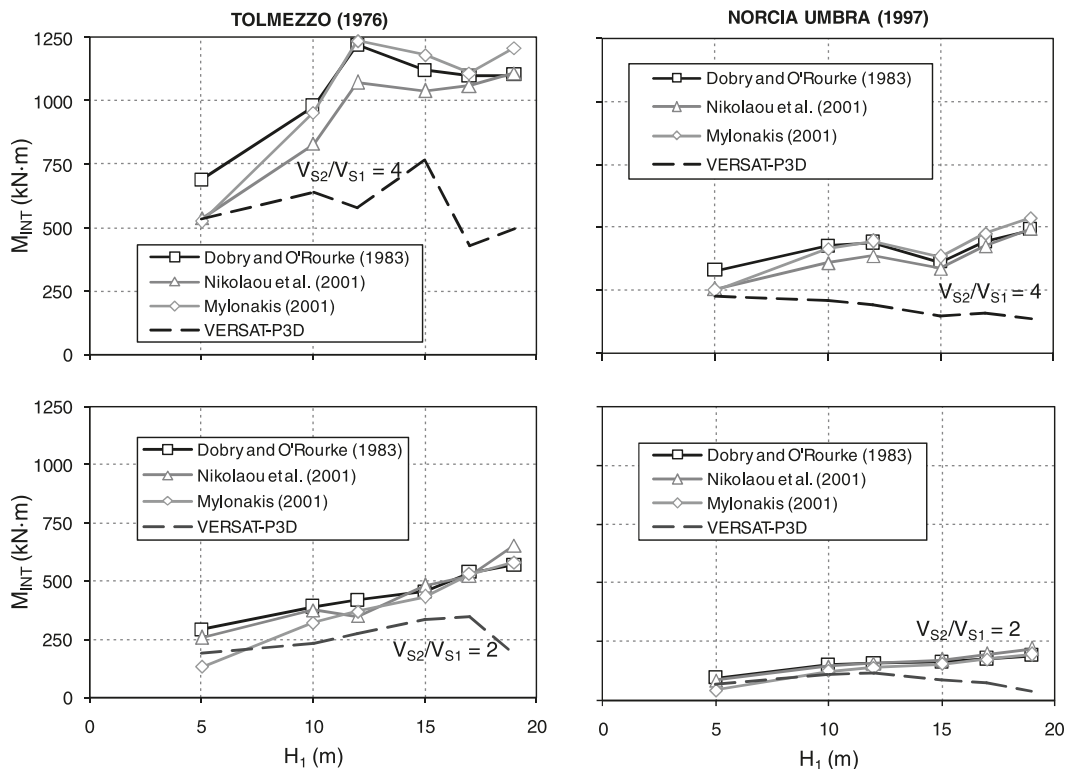


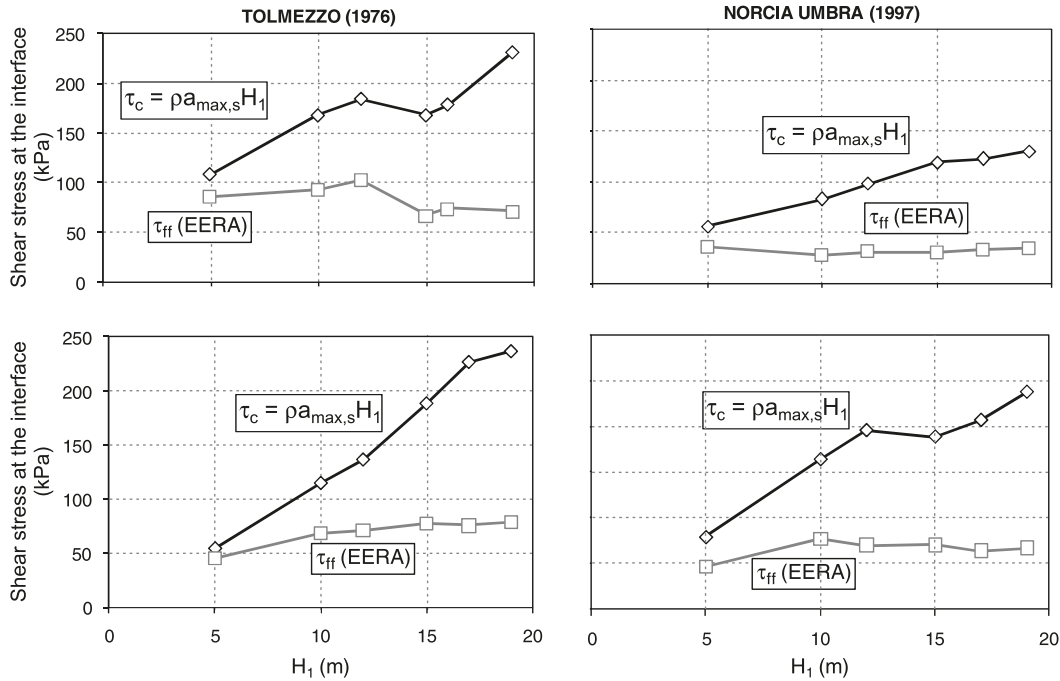
**Fig. 8.** Comparison between bending moments predicted by analytical solutions and those evaluated by the finite element analyses for subsoils S1 and S2 ( $V_{S1} = 50$  m/s).



the plot of the bending moments evaluated by the finite element analyses (see Fig. 5). This suggests a possible correlation between the bending moments evaluated by VERSAT-

P3D and the maximum shear stress  $\tau_{ff}$  (or strain  $\gamma_{1ff}$ ) computed by the free-field analyses performed via EERA. In this respect, the original closed-form expression provided

Fig. 9. Maximum shear stress at the interface between the two layers in the case  $V_{s1} = 100$  m/s.



by Nikolaou et al. (2001) or alternatively the one by Mylonakis (2001) will be used as the rational basis of this potential correlation.

The closed-form expression suggested by Mylonakis (2001) (eq. [10]) can be put in the form

$$[18] \quad M/a = \Phi \gamma_1$$

where  $\Phi$  is equal to 1 in the pseudostatic form of the original Mylonakis' approach and  $a$  is a coefficient independent of the seismic excitation

$$[19] \quad a = (E_p I_p) \left( \frac{\epsilon_p}{\gamma_1} \right) \frac{1}{r}$$

Figure 10 illustrates the plot of the ratio  $M_V/a$ , where  $M_V$  is the bending moment computed by VERSAT-P3D, against the peak shear strain  $\gamma_{1ff}$ .

The linear regression in this plane provides  $\Phi = 1.30$ . Even if there is an evident relationship between  $M_V$  and  $\gamma_{1ff}$ , there are cases for which this linear correlation is not satisfactory. This can be attributed to the hypothesis of thick layers adopted by Mylonakis (2001) to develop the theoretical solution synthesized by eq. [10]. As a consequence of this hypothesis, the method is intrinsically unable to provide accurate results when the interface between the two layers is in the vicinity of the pile base or the pile head. As shown in Fig. 11, a very substantial improvement in the accuracy of the correlation between  $M_V$  and  $\gamma_{1ff}$  is obtained when considering only the points corresponding to cases with  $H_1$  ranging between  $L_{a1}$  and  $L - L_{a2}$ , with  $L_{a1}$  and  $L_{a2}$  being, respectively, the "active pile length" in the upper and in the lower layer (as defined by Mylonakis 2001). In this case, the linear regression provides a correlation coefficient  $\Phi = 1.32$ . In the same plane, the curves  $M_V/a \pm \sigma$  (where  $\sigma$  is the standard deviation) have been also reported for comparison.

The static-to-dynamic transformation factor  $\Phi$  included in the formula of Mylonakis (2001) (eq. [18]) accounts for the effect of frequency on the strain-transmissibility. However, in the model developed by Mylonakis (2001) the dynamic excitation has the form of horizontal harmonic displacements imposed at the base of the soil profile, while that proposed in the present work ( $\Phi = 1.32$ ) is an overall coefficient calibrated by a curve-fitting operation of numerical data computed in the time domain. In this sense, the amplification factor introduced by Mylonakis is not perfectly equivalent to that included in eq. [18]. For both the Mylonakis' method and eq. [18], the coefficient  $\Phi$  represents the effect of the dynamic nature of the excitation on the percentage of  $\gamma_1$  that is transmitted to the pile in the form of bending strain, so that the same symbol may be retained.

For cases where the hypothesis of "thick layers" is satisfied, it may be convenient to perform separate curve-fitting for resonant and nonresonant conditions. The condition of resonance corresponds to the case where the fundamental natural period of the deposit falls within the range of predominant periods of the excitation. In this respect, this interval of periods has been defined on the Fourier amplitude spectrum as that corresponding to the range over which  $1/\sqrt{2}$  times the maximum Fourier amplitude spectrum is exceeded (Kramer 1996). For the earthquakes employed in the analyses, resonance occurs for subsoil profiles belonging to group S4 ( $V_{s1} = 100$  m/s,  $V_{s2}/V_{s1} = 4$ ) and particularly for  $H_1/L$  ranging between 0.25 and 0.85 (see Table 1).

A new fitting is then performed for the nonresonant profiles. This gives a correlation coefficient  $\Phi$  equal to 1.30, which is slightly lower than the value of 1.32. For resonant subsoil profiles, the linear correlation between  $M_V/a$  and  $\gamma_{1ff}$  gives  $\Phi = 1.39$ , which is slightly larger than 1.32.

The same procedure adopted for the Mylonakis' method (Mylonakis 2001) can be applied for the closed form expres-

**Fig. 10.** Plot of  $M_V/a$  against  $\gamma_{1ff}$ .

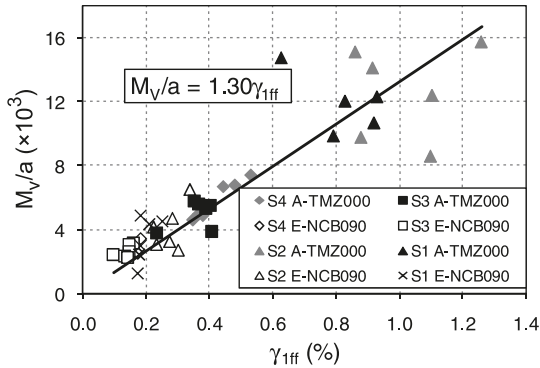
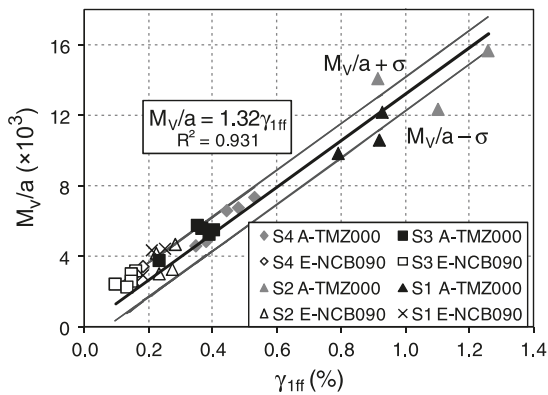


**Fig. 11.** Plot of  $M_V/a$  versus  $\gamma_{1ff}$  with the exception of the cases for which  $H_1$  is within the active pile length  $L_{a1}$  or  $L_{a2}$ .



sion of Nikolaou et al. (2001). Indeed, eq. [8] can be put in the form

$$[20] \quad \frac{M}{b} = \beta \tau_c$$

where  $\beta = 0.042$  in the original expression of Nikolaou et al. (2001) and  $b$  is a coefficient independent of the earthquake excitation

$$[21] \quad b = d^3 \left(\frac{L}{d}\right)^{0.3} \left(\frac{E_p}{E_1}\right)^{0.65} \left(\frac{V_{s2}}{V_{s1}}\right)^{0.5}$$

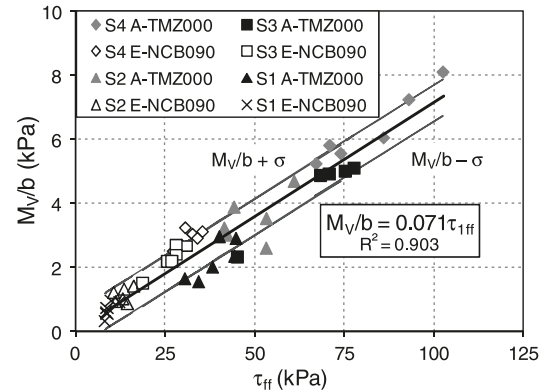
In Fig. 12, the ratios  $M_V/b$  are plotted against the peak shear stress  $\tau_{ff}$ . In this case, all data can be fitted with satisfactory accuracy by the linear regression

$$[22] \quad \frac{M_V}{b} = 0.071 \tau_{ff}$$

The curves  $M_V/b \pm \sigma$  have been also reported for comparison. It appears beneficial, again, to account for the effect of frequency by distinguishing between resonant and nonresonant conditions. The linear correlation coefficient  $\beta$  is slightly smaller than 0.071 for nonresonant profiles ( $\beta = 0.069$ ). For resonant profiles, this coefficient is slightly larger ( $\beta = 0.075$ ), as was expected. At a preliminary stage it may be sufficient to assume  $\beta = 0.071$  as an average dynamic coefficient.

A modified criterion for assessment of the kinematic pile bending moments at the interface between two layers is therefore suggested. This involves the following steps:

**Fig. 12.** Plot of  $M_V/b$  versus the maximum shear stress at the interface  $\tau_{1ff}$ .



- (1) Perform a preliminary analysis of the free-field response to evaluate  $\tau_{ff}$  at the interface.
- (2) Establish whether resonance does or does not occur.
- (3) Evaluate the maximum bending moment at the interface with the following equation (adapted from Nikolaou et al. 2001)

$$[23] \quad M = \beta d^3 \left(\frac{L}{d}\right)^{0.3} \left(\frac{E_p}{E_1}\right)^{0.65} \left(\frac{V_{s2}}{V_{s1}}\right)^{0.5} \tau_{ff}$$

As shear stress tends to saturate with increasing level of shaking, thus being an inappropriate quantity to describe inelastic soil behaviour, it may be convenient to express the bending moment as a function of actual peak shear strain  $\gamma_{1ff}$ . Equation [23] can be then put in the form

$$[24] \quad M = \beta G_1 d^3 \left(\frac{L}{d}\right)^{0.3} \left(\frac{E_p}{E_1}\right)^{0.65} \left(\frac{V_{s2}}{V_{s1}}\right)^{0.5} \gamma_{1ff}$$

Finally, rearranging eq. [24] gives

$$[25] \quad M = \frac{0.5}{1 + \nu} \beta d^3 E_p \left(\frac{L}{d}\right)^{0.3} \left(\frac{E_p}{E_1}\right)^{-0.35} \left(\frac{V_{s2}}{V_{s1}}\right)^{0.5} \gamma_{1ff}$$

with  $\beta$  being a coefficient that depends on the occurrence of resonance.

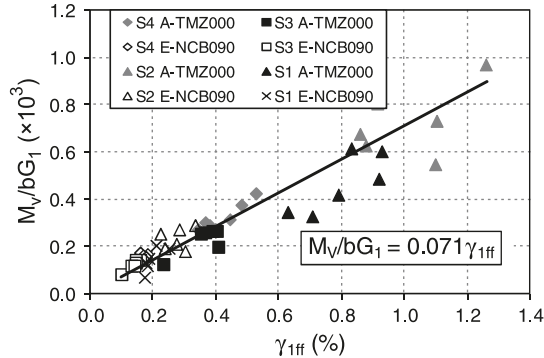
The bending moment values  $M_V$ , normalized to the quantity  $(bG_1)$ , have been plotted in Fig. 13 against the actual peak shear strain  $\gamma_{1ff}$ .

A calculation example for both eqs. [18] and [25] is reported in Appendix A.

## Conclusions

Seismically loaded piles are traditionally designed to resist only the inertial bending moments generated from the oscillation of the superstructure, thus neglecting the effect of kinematic interaction between the pile and the soil. It is only in recent times that the kinematic effects have received adequate attention by code and provisions such as Eurocode EN1998-5 (CEN/TC 250 2003b) and the new Italian regulation (Consiglio Superiore dei Lavori Pubblici 2008). Based on the studies carried out on BDWF models, a number of simplified procedures are available in published literature

**Fig. 13.** Plot of  $M_V/bG_1$  versus the actual peak shear stress at the interface  $\gamma_{1ff}$ .



for a first evaluation of kinematic bending moments at the interface between two layers.

A comprehensive parametric study was presented for kinematic bending moments of piles in layered soil deposits. The study has focused on somewhat simplified conditions, such as vertically propagating SH waves, two-layer subsoil underlain by a rigid base, linear-elastic soil behaviour, and shear-strain-independent soil damping. Despite these assumptions and the limited number of earthquake events employed in the analyses, the paper highlights a number of fundamental issues about the kinematic response of piles under transient earthquake excitations.

Group effects due to kinematic interaction have found to be negligible, in agreement with analytical studies and field recordings published in literature. The study has been therefore focused on the kinematic response of single piles. It has been shown that the simplified methods available in literature may not be suitable for all subsoil conditions examined in the present paper. Two modified criteria to evaluate the maximum pile bending moment at an interface between two soil layers have been suggested (eqs. [18] and [25]). These are based on modified expressions of the methods proposed by Mylonakis (2001) and Nikolaou et al. (2001). The criterion modified from Nikolaou et al. (2001) is fundamentally different from the original method as it requires a preliminary assessment of the peak soil shear strain via a free-field site response analysis. While the criterion adapted from the mechanistic model developed by Mylonakis (2001) may lose accuracy when the hypothesis of thick layers is not satisfied, the criterion modified from Nikolaou et al. (2001) (eq. [25]) has general applicability to engineering problems and can be considered a rational enhancement of the simplified methods available in published literature.

## Acknowledgements

This research has been developed under the auspices of the research project ReLUIIS “Innovative methods for the design of geotechnical systems under earthquake excitation”, funded by Dipartimento della Protezione Civile (National Emergency Management Agency).

## References

Bardet, J.P., Ichii, K., and Lin, C.H. 2000. EERA: a computer program for equivalent-linear earthquake site response analyses of

layered soil deposits. Department of Civil Engineering, University of Southern California, Los Angeles, Calif. Available from [geoinfo.usc.edu/geees](http://geoinfo.usc.edu/geees).

- Bentley, K.J., and El Naggar, M.H. 2000. Numerical analysis of kinematic response of single piles. *Canadian Geotechnical Journal*, **37**(6): 1368–1382. doi:10.1139/cgj-37-6-1368.
- Building Seismic Safety Council. 2003. NEHRP recommended provisions for seismic regulations for new buildings and other structures (FEMA 450). National Earthquake Hazards Reduction Program (NEHRP), Building Seismic Safety Council, Washington, D.C.
- CEN/TC 250. 2003a. Eurocode 8: Design of structures for earthquake resistance Part 1: General Rules, seismic actions and rules for buildings. Standard EN-1998-1. European Committee for Standardization Technical Committee 250 (CEN/TC 250), Brussels, Belgium.
- CEN/TC 250. 2003b. Eurocode 8: Design of structures for earthquake resistance Part 5: Foundations, retaining structures and geotechnical aspects. Standard EN-1998-5. European Committee for Standardization Technical Committee 250 (CEN/TC 250), Brussels, Belgium.
- Consiglio Superiore dei Lavori Pubblici. 2008. Approvazione delle nuove norme tecniche per le costruzioni. DM 14.01. Gazzetta Ufficiale della Repubblica Italiana, No. 29, 4 February 2008. [In Italian.]
- Dobry, R., and O’Rourke, M.J. 1983. Discussion on ‘Seismic response of end-bearing piles’ by R. Flores-Berrones and R.V. Whitman. *Journal of the Geotechnical Engineering Division*, **109**(5): 778–781. doi:10.1061/(ASCE)0733-9410(1983)109:5(778).
- Fan, K., Gazetas, G., Kaynia, A., Kausel, E., and Ahmad, S. 1991. Kinematic seismic response of single piles and pile groups. *Journal of the Geotechnical Engineering Division*, **117**(12): 1860–1879. doi:10.1061/(ASCE)0733-9410(1991)117:12(1860).
- Finn, W.D.L. 2005. A study of piles during earthquakes: Issues of design and analysis. *Bulletin of Earthquake Engineering*, **3**(2): 141–234. doi:10.1007/s10518-005-1241-3.
- Gazetas, G., Tazoh, T., Shimizu, K., and Fan, K. 1993. Seismic response of the pile foundation of the Ohba-Ohashi Bridge. *In Proceedings of the 3rd International Conference on Case Histories in Geotechnical Engineering*, St. Louis, Mo., 1–6 June 1993. Edited by S. Prakash. University of Missouri–Rolla, Rolla, Mo. Vol. 3. pp. 1803–1809.
- Kavvas, M., and Gazetas, G. 1993. Kinematic seismic response and bending of free-head piles in layered soil. *Géotechnique*, **43**(2): 207–222.
- Kaynia, A. 1997. Earthquake-induced forces in piles in layered media. *Geotechnical Special Publication 70*. American Society of Civil Engineers (ASCE), New York. pp. 75–95.
- Kaynia, A.M., and Mahzooni, S. 1996. Forces in pile foundations under seismic loading. *Journal of Engineering Mechanics*, **122**(1): 46–53. doi:10.1061/(ASCE)0733-9399(1996)122:1(46).
- Kramer, S.L. 1996. *Geotechnical earthquake engineering*. Prentice-Hall, Upper Saddle River, N.J.
- Lysmer, J., and Kuhlemeyer, R.L. 1969. Finite dynamic model for infinite media. *Journal of the Engineering Mechanics Division*, ASCE, **95**(EM4): 859–877.
- Maheshwari, B.K., Truman, K.Z., El Naggar, M.H., and Gould, P.L. 2004. Three-dimensional finite element nonlinear dynamic analysis of pile groups for lateral transient and seismic excitations. *Canadian Geotechnical Journal*, **41**(1): 118–133. doi:10.1139/t03-073.
- Maheshwari, B.K., Truman, K.Z., Gould, P.L., and El Naggar, M.H. 2005. Three-dimensional nonlinear seismic analysis of single piles using finite element model: effect of plasticity of soil.

International Journal of Geomechanics, **5**(1): 35–44. doi:10.1061/(ASCE)1532-3641(2005)5:1(35).

Maiorano, R.M.S., and Aversa, S. 2006. Importanza relativa di interazione cinematica ed inerziale nell'analisi dei pali di fondazione sotto azioni sismiche. In *Atti del V Convegno Nazionale dei Ricercatori di Geotecnica*, Bari, Italy, 15–16 September 2006. Hevelius ed., Benevento, Italy. pp. 393–414. [In Italian.]

Maiorano, R.M.S., Aversa, S., and Wu, G. 2007. Effects of soil non-linearity on bending moments in piles due to seismic kinematic interaction. In *Proceedings of the 4th International Conference on Earthquake Geotechnical Engineering*, Thessaloniki, Greece, 25–28 June 2007. Springer, New York. Paper No. 1574.

Margason, E., and Holloway, D.M. 1977. Pile design during earthquakes. In *Proceedings of the 6th World Conference on Earthquake Engineering*, New Delhi, India, 10–14 January 1977. Sarita Prakashan, Meerut, India. pp. 237–243.

Mylonakis, G. 2001. Simplified model for seismic pile bending at soil layer interfaces. *Soils and Foundations*, **41**(4): 47–58.

Nikolaou, A.S., and Gazetas, G. 1997. Seismic design procedure for kinematically loaded piles. In *Proceedings of the 14th International Conference on Soil Mechanics and Foundation Engineering*, Hamburg, Germany, 6–12 September 1997. Special volume: ISSMFE TC4 Earthquake geotechnical engineering. Balkema, Rotterdam, the Netherlands. pp. 253–260.

Nikolaou, A.S., Mylonakis, G., Gazetas, G., and Tazoh, T. 2001. Kinematic pile bending during earthquakes analysis and field measurements. *Géotechnique*, **51**(5): 425–440. doi:10.1680/geot.51.5.425.39973.

Pender, M. 1993. Aseismic pile foundation design analysis. *Bulletin of the New Zealand National Society for Earthquake Engineering*. **26**(1): 49–160.

Presidenza del Consiglio dei Ministri. 2003. Primi elementi in materia di criteri generali per la classificazione sismica del territorio nazionale e di normative tecniche per le costruzioni in zona sismica. OPCM-3274. *Gazzetta Ufficiale della Repubblica Italiana*, No. 105, 8 May 2003. [In Italian.]

Randolph, M.F. 1981. Response of flexible piles to lateral loading. *Géotechnique*, **31**(2): 247–259.

Scasserra, G., Lanzo, G., Mollaioli, F., Stewart, J.P., Bazzurro, P., and Decanini, L.D. 2006. Preliminary comparison of ground motions from earthquakes in Italy with ground motion prediction equations for active tectonic regions. In *Proceedings of the 8th U.S. National Conference on Earthquake Engineering*, San Francisco, Calif., 18–22 April 2006. [CD-ROM]. Mira Publishing, San Francisco, Calif. Paper No. 1824.

Seed, H.B., and Idriss, I.M. 1982. Ground motions and soil liquefaction during earthquakes. *Earthquake Engineering Research Institute Monograph*. University of California, Berkeley, Calif.

Seed, H.B., Wong, R.T., Idriss, I.M., and Tokimatsu, K. 1986. Moduli and damping factors for dynamic analyses of cohesionless soils. *Journal of Geotechnical Engineering*, **112**(11): 1016–1032. doi:10.1061/(ASCE)0733-9410(1986)112:11(1016).

Sica, S., Mylonakis, G., and Simonelli, A.L. 2007. Kinematic bending of piles: analysis vs. code provisions. In *Proceedings of the 4th International Conference on Earthquake Geotechnical Engineering*, Thessaloniki, Greece, 25–28 June 2007. Springer, New York. Paper No. 1674.

Wu, G. 2006. VERSAT-P3D: Quasi-3D dynamic finite element analysis of single piles and pile groups. Version 2006 [computer program]. 2000–2006 Wutec Geotechnical International, Vancouver, B.C.

Wu, G., and Finn, W.D.L. 1997a. Dynamic elastic analysis of pile foundations using finite element method in the frequency do-

main. *Canadian Geotechnical Journal*, **34**(1): 34–43. doi:10.1139/cgj-34-1-34.

Wu, G., and Finn, W.D.L. 1997b. Dynamic nonlinear analysis of pile foundations using finite element method in the time domain. *Canadian Geotechnical Journal*, **34**(1): 44–52. doi:10.1139/cgj-34-1-44.

### List of symbols

$a_{ff}$ , $a_{ff}(z, t)$	free-field soil acceleration
$a_g$	base rock acceleration
$a_{max}$	maximum acceleration at any given depth
$a_{max,s}$	maximum acceleration at the soil surface
$a, b$	coefficients independent of the earthquake excitation
$B$	foundation width
$[C]$	damping matrix
$c$	ratio of shear moduli of the soil layers
$D$	hysteretic damping ratio
$d$	diameter of pile
$E$	Young's modulus
$E_1$	Young's modulus of soil layer 1
$E_p$	Young's modulus of pile
$F$	dimensionless function of the ratio of the shear moduli of two layers
$G_0$	small strain shear modulus of soil
$G_1, G_2$	shear modulus of soil layers 1 and 2, respectively
$H$	depth of the bedrock roof
$H_1, H_2$	thickness of soil layers 1 and 2, respectively
$h_i$	thickness of layer $i$
$\{I\}$	unit column vector
$I_p$	inertia of pile
$[K]$	stiffness matrix
$k$	soil spring stiffness
$k_1$	soil spring stiffness for layer 1
$L$	length of pile
$L_{a1}, L_{a2}$	"active pile length" in the upper and lower layer, respectively
$M, M(z, t)$	pile bending moment
$[M]$	mass matrix
$M_{CAP}$	maximum bending moment at the pile top
$M_{INT}$	maximum bending moment at the interface depth
$M_V$	maximum bending moment at the interface obtained by FE analyses
$M_w$	magnitude of seismic event
$n$	number of layers
$1/R(z, t)$	curvature
$R^2$	squared correlation coefficient
$r$	pile radius
$r_d$	depth factor
$s$	pile spacing
$t$	time
$u$	horizontal displacement
$V_s$	shear wave velocity of soil
$V_{s1}, V_{s2}$	shear wave velocities in layers 1 and 2, respectively
$V_{s,30}$	equivalent velocity
$V_{si}$	shear-wave velocity of layer $i$
$\{\ddot{v}\}, \{\dot{v}\}, \{v\}$	the nodal acceleration, velocity, and displacement, respectively
$\ddot{v}_0(t)$	base acceleration
$z$	depth from the ground surface
$\beta$	linear regression factor
$\gamma_1, \gamma_2$	shear strain in the upper and lower layer, at the interface depth
$\gamma_{1ff}$	maximum shear strain computed by the free-field analyses

$\delta$	dimensionless parameter relating $k$ and $E$
$\varepsilon_p$	pile bending strain
$\theta$	variable to improve the stability and the accuracy of the integration method
$\nu$	Poisson's ratio
$\rho$	soil density
$\rho_1$	density of upper layer
$\Phi$	frequency factor
$\sigma$	standard deviation
$\tau_{ff}$	maximum shear stress computed by the free-field analyses
$\tau$	static shear stress of the soil
$\tau_C$	characteristic shear stress
$\omega$	circular frequency
$\omega_1$	fundamental circular frequency of the pile-soil system

## Appendix A. Calculation example

Consider the subsoil profile S3-4 (see Table 1), the 1976 Tolmezzo earthquake, and a pile 0.6 m in diameter with a length of 20 m. Let the Poisson's coefficient  $\nu$  be 0.4 for both the upper and lower layers. The calculation will be performed for both eq. [18] adapted from Mylonakis (2001) and eq. [25] modified from Nikolaou et al. (2001). The kinematic bending moment computed by VERSAT-P3D (Wu 2006) is equal to 240 kN-m.

For the case under examination

$$E_p = 25 \times 10^4 \text{ MPa}$$

$$I_p = 0.00636 \text{ m}^4$$

$$c = (G_2/G_1)^{1/4} = \sqrt{2}$$

The active lengths of the upper and lower layer are, respectively:

$$L_{a1} = 4.17 \text{ m} \quad \text{and} \quad L_{a2} = 2.95 \text{ m}$$

The interface  $H_1$  falls between  $L_{a1}$  and  $L - L_{a2}$  and therefore, based on the results summarized in the graph of Fig. 11, eq. [18] can be certainly considered appropriate.

From eqs. [13] and [12], respectively, it is possible to calculate  $\delta$  and  $k_1$

$$\delta = 2.54$$

$$k_1 = 138 \text{ MPa}$$

Substituting into the pseudostatic expression of the strain transmissibility (eq. [11]) gives

$$\varepsilon_p/\gamma_1 = 0.082$$

The maximum shear strain at the interface level computed from the free-field analysis is

$$\gamma_{1ff} = 0.4\%$$

The fundamental natural period of the deposit ( $T_p = 0.80$  s) falls outside the range of the predominant periods of the signal ( $T_{p1} = 0.26$  s and  $T_{p2} = 0.53$  s), thus, for this subsoil there is no resonance. The dynamic coefficient  $\Phi$  can therefore be set equal to 1.30.

In this case, eq. [18], adapted from Mylonakis (2001), gives

$$M = 254 \text{ kN-m}$$

As there is no resonance, the correlation coefficient  $\beta$  can be set equal to 0.069. The actual peak shear strain has already been computed for eq. [18] and is  $\gamma_{1ff} = 0.4\%$ . By substituting this in to eq. [25], the maximum kinematic bending moment is

$$M = 229 \text{ kN-m}$$

## References

- Mylonakis, G. 2001. Simplified model for seismic pile bending at soil layer interfaces. *Soils and Foundations*, **41**(4): 47–58.
- Nikolaou, A.S., Mylonakis, G., Gazetas, G., and Tazoh, T. 2001. Kinematic pile bending during earthquakes analysis and field measurements. *Géotechnique*, **51**(5): 425–440. doi:10.1680/geot.51.5.425.39973.
- Wu, G. 2006. VERSAT-P3D: Quasi-3D dynamic finite element analysis of single piles and pile groups. Version 2006 [computer program]. 2000–2006 Wutec Geotechnical International, Vancouver, B.C.

## List of symbols

$c$	ratio of shear moduli of the soil layers
$E$	Young's modulus
$E_p$	Young's modulus of pile
$G_1, G_2$	shear modulus of soil layers 1 and 2, respectively
$H_1$	thickness of soil layer 1
$I_p$	inertia of pile
$k$	soil spring stiffness
$k_1$	soil spring stiffness for layer 1
$L$	length of the pile
$L_{a1}, L_{a2}$	"active pile length" in the upper and lower layers, respectively
$M$	pile bending moment
$T_p$	fundamental natural period of the deposit
$T_{p1}, T_{p2}$	predominant periods of the signal
$\beta$	linear regression factor
$\gamma_1$	shear strain in the upper layer at the interface depth
$\gamma_{1ff}$	maximum shear strain computed by the free-field analyses
$\delta$	dimensionless parameter relating $k$ and $E$
$\varepsilon_p$	pile bending strain
$\nu$	Poisson's ratio
$\Phi$	frequency factor